http://www.jstage.jst.go.jp/browse/biophysics

BIOPHYSICS

Vol. 10, pp. 35–41 (2014)
doi: 10.2142/biophysics.10.35

Effect of the MotB(D33N) mutation on stator assembly and rotation of the proton-driven bacterial flagellar motor

Shuichi Nakamura[1], Tohru Minamino[2], Nobunori Kami-ike[2], Seishi Kudo[1] and Keiichi Namba[2,3]

[1]*Department of Applied Physics, Graduate School of Engineering, Tohoku University, 6-6-05 Aoba, Aoba-ku, Sendai 980-8579, Japan*
[2]*Graduate School of Frontier Bioscience, Osaka University, 1-3 Yamadaoka, Suita, Osaka 565-0871, Japan*
[3]*Riken Quantitative Biology Center, 1-3 Yamadaoka, Suita, Osaka 565-0871, Japan*

Received April 1, 2014; accepted May 28, 2014

The bacterial flagellar motor generates torque by converting the energy of proton translocation through the transmembrane proton channel of the stator complex formed by MotA and MotB. The MotA/B complex is thought to be anchored to the peptidoglycan (PG) layer through the PG-binding domain of MotB to act as the stator. The stator units dynamically associate with and dissociate from the motor during flagellar motor rotation, and an electrostatic interaction between MotA and a rotor protein FliG is required for efficient stator assembly. However, the association and dissociation mechanism of the stator units still remains unclear. In this study, we analyzed the speed fluctuation of the flagellar motor of *Salmonella enterica* wild-type cells carrying a plasmid encoding a nonfunctional stator complex, MotA/B(D33N), which lost the proton conductivity. The wild-type motor rotated stably but the motor speed fluctuated considerably when the expression level of MotA/B(D33N) was relatively high compared to MotA/B. Rapid accelerations and decelerations were frequently observed. A quantitative analysis of the speed fluctuation and a model simulation suggested that the MotA/B(D33N) stator retains the ability to associate with the motor at a low affinity but dissociates more rapidly than the MotA/B stator. We propose that the stator dissociation process depends on proton translocation through the proton channel.

Key words: *Salmonella*, stator, torque generation, proton channel, speed fluctuation

Corresponding authors: Shuichi Nakamura, Department of Applied Physics, Graduate School of Engineering, Tohoku University, 6-6-05 Aoba, Aramaki, Aoba-ku, Sendai 980-8579, Japan. e-mail: naka@bp.apph.tohoku.ac.jp; Keiichi Namba, Graduate School of Frontier Biosciences, Osaka University, 1-3 Yamadaoka, Suita, Osaka 565-0871, Japan. e-mail: keiichi@fbs.osaka-u.ac.jp

The bacterial flagellar motor, which is embedded in the cytoplasmic membrane, is a rotary molecular nanomachine driven by the electrochemical potential difference of specific cations across the cytoplasmic membrane. Five flagellar proteins, FliG, FliM, FliN, MotA and MotB, are involved in motor rotation. FliG, FliM, and FliN form a ring structure called the C ring, which is involved in switching the rotational direction. Four copies of MotA and two copies of MotB form a stator complex, which acts as a proton translocation channel across the cytoplasmic membrane[1–5]. A structural change of the cytoplasmic loop of MotA induced by protonation of a highly conserved aspartic acid residue of MotB, Asp-33, is thought to cause electrostatic interactions between MotA and FliG at the stator-rotor interface[6-9]. Two prolyl residues of MotA, Pro-173 and Pro-222, have been proposed to be critical for the energy coupling mechanism[8,10]. It has been shown that Pro-173 facilitates proton dissociation from the proton-binding site of MotB to the cytoplasm[11]. Arg-90 and Glu-98 of MotA are thought to interact electrostatically with conserved charged residues located in the C-terminal domain of FliG[12–15]. Direct observations of the elementary process of the torque generation cycle indicate that the motor containing a single stator unit makes 26 steps per revolution, which is consistent with the number of FliG subunits forming the rotor ring structure[16,17].

Overexpression of *Salmonella* MotA significantly reduces motility of wild-type cells, suggesting that MotA alone can be incorporated into the motor[14]. The R90E and E98K substitutions in *Salmonella* MotA abolish the subcellular localization of GFP-MotB[14]. The FliG(D289K) and FliG(R281V) mutations, which partially restore the motility of the *motA*(R90E) and *motA*(E98K) mutants, respectively[7], sig-

nificantly reduce the probability of GFP-MotB localization to the motor as well[15]. These suggest that electrostatic interactions between MotA Arg-90 and FliG Asp-289 and between MotA Glu-98 and FliG Arg-281 are required for efficient stator assembly around the rotor[14,15].

At least 11 copies of the MotA/MotB (hereafter MotA/B) complex are incorporated around the rotor to be the stators[18]. Since MotB contains a highly conserved peptidoglycan-binding (PGB) motif in its C-terminal domain ($MotB_c$), the MotA/B complex is thought to be anchored around the rotor through the PGB motif[19–22]. High resolution single molecule imaging techniques has shown the turnover of GFP-fused stator unit between the motor and the membrane pool during rotation, providing evidence that the stator unit is not always kept anchored to each specific binding site but goes through a rather dynamic association/dissociation process[23]. Recently, it has been shown that the flagellar motor responds to changes in external load to control the number of functional stators in the motor[24,25] and that $MotB_C$ acts as a load-sensitive structural switch to regulate the assembly and disassembly cycle of the stators in response to the load changes[26]. Interestingly, the MotA/B complex senses even a small change in the external load to regulate its proton conductivity during flagellar motor rotation[27].

MotB(D33N) and MotA still forms the stator complex but the proton conductivity is lost and therefore the complex is non-functional as the stator[6,8,28]. The MotA/B(D33N) complex exerts a strong dominant negative effect on the motility of wild-type cells in *Salmonella*. This is in agreement with the observation by an epi-illumination fluorescence microscopy that GFP-fused MotB(D33N) is localized to the flagellar motor[14]. These suggest that the MotA/B(D33N) complex lacking the proton conductivity can be incorporated into the motor. Interestingly, over-expression of the MotA/B(D33N) complex reduces the number of functional stators to one or two but not to zero[17]. Yet, the maximum speed of the motor with many non-functional MotA/B(D33N) stators is almost at the wild-type level under low load[17]. These observations raise the possibility that the D33N mutation reduces the binding affinity of the MotA/B complex for the motor compared to the wild-type.

In the present study, we investigated the effect of the non-functional stator unit MotA/B(D33N) on flagellar motor rotation of *Salmonella* wild-type cells and showed that the speed fluctuation became large with an increase in the expression level of MotA/B(D33N). Abrupt acceleration, deceleration and pausing were observed during the rotation. The motor kept rotating even when the expression level of MotA/B(D33N) was increased up to ten times of MotA/B. These observations together with model simulation suggest that the D33N mutation markedly reduces the binding affinity of the stator for the rotor and makes the rate of stator detachment from the rotor much faster than that of the wild-type stator.

Materials and Methods

Bacterial strains, plasmids, media

A *Salmonella* strain, SJW46(*fliC*(Δ204–292))[29], was used in this study. This strain has intact flagellar motors with sticky flagellar filaments and chemotaxis system. A plasmid, pNSK9-D33N, encodes wild-type MotA and MotB(D33N) on pTrc99A (Pharmacia)[17]. Luria broth (LB) and motility buffer were prepared as described before[30].

Bead assay

Overnight culture of SJW46 cells transformed with pTrc99A or pNSK9-D33N was diluted into fresh LB with or without IPTG and incubated for 4 h at 37°C. Bead assays were carried out as previously described[31]. The position of 1-μm bead attached on the sticky filament of SJW46 was determined by a quadrant photodiode at 1-ms intervals. The average value and the standard deviation of rotation rate were calculated according to Muramoto *et al*[32]. The rotational diffusions of the flagellar filament with bead were calculated as described before[33,34]. The instrumental uncertainty was also calculated as described before[33,34], which was evaluated from the rotation rate and a half of the sampling interval.

Immunoblotting

SJW46 carrying pTrc99A or pNSK9-D33N was grown in LB under the same condition with the bead assay. Cultures were centrifuged to obtain cell pellets. The cell pellets were resuspended in SDS-loading buffer, normalized in cell density to give a constant amount of cells. Immunoblotting using polyclonal anti-MotB antibody was carried out as previously described[35].

Computer simulation

Computer simulation was performed by a simple kinetic model proposed before[32] (see Computer simulation in Result). Kinetic parameters were manually optimized to reproduce experimental results. The sampling interval in the simulation was the same as that of the bead assays (1 ms), and the expression level of the stator complex is based on the result of immunoblotting. All calculations were performed using a macro developed in Microsoft Excel.

Results

Speed fluctuation of *Salmonella* flagellar motor

When MotA/B(D33N) was expressed in the wild-type cell, a much higher expression level than that of MotA/B was required to reduce the number of functional stators around the rotor to one or two[17]. This indicated that the binding affinity of the MotA/B(D33N) complex for the rotor is much lower than that of the wild-type MotA/B complex. To test this, we changed the expression level of the MotA/B(D33N) complex in the *Salmonella* SJW46 cell,

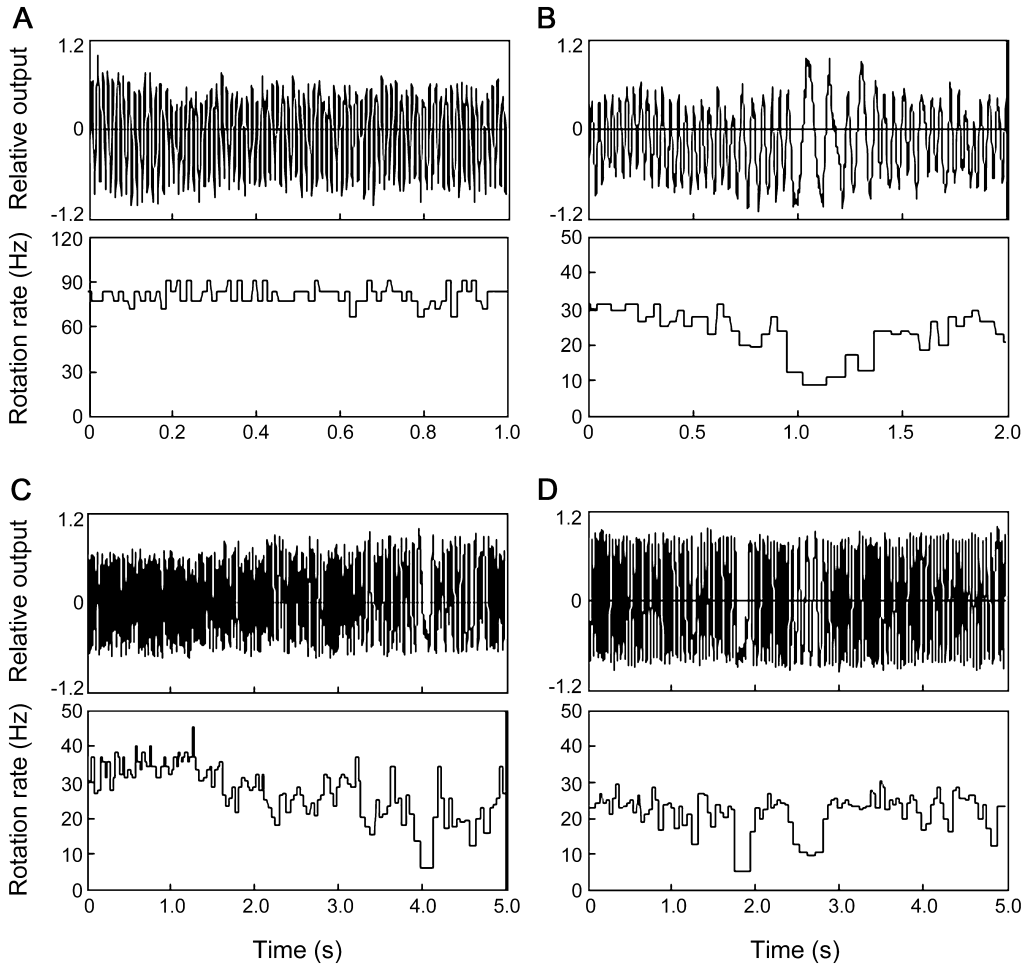

Figure 1 Speed fluctuations of the wild-type and MotA/B(D33N)-stator containing flagellar motors. Temporal records of motor rotation measurement by bead assay for wild-type cells carrying a vector plasmid (pTrc99A) (A), for wild-type cells over-expressing MotA/B(D33N) without adding IPTG (B and C), and for wild-type cells over-expressing MotA/B(D33N) by adding 10 μM IPTG (D). The average speeds and standard deviations are (A) 77.5±8.5 Hz, (B) 25.2±6.3 Hz, (C) 26.5±7.7 Hz, and (D) 21.1±5.6 Hz. The cells carrying a plasmid encoding MotA/B(D33N) were grown with 10 μM IPTG. The rotation rate was determined from the peak intervals of the temporal records of bead positions in the upper panel.

which produces the wild-type motor and sticky filaments, and analyzed the motor performance by bead assays.

Figure 1 shows the rotation of the *Salmonella* flagellar motor with a 1-μm polystyrene bead. The motor of the cell carrying a vector pTrc99A (wild-type stator) stably rotated at an average speed (<ω>) of 77.5 Hz with a standard deviation (σ_ω) of 8.5 Hz. The speed fluctuation, evaluated as the value of $\sigma_\omega/<\omega>$ as described before[32], was 0.11 (Fig. 1A). On the other hand, the motor of the cell carrying a plasmid pNSK9-D33N rotated much more slowly with large fluctuations in speed. A few typical examples are shown in Figure 1B and C, in which no IPTG was added. The average speed was around 30 Hz and the speed fluctuation was around 6 Hz ($\sigma_\omega/<\omega> = 0.20$). The average speed became even lower and the speed fluctuation became larger when the expression level of the mutant stator was increased by adding 10 μM IPTG (Fig. 1D). The average speed was 21.1 Hz and the standard deviation was 5.6 Hz ($\sigma_\omega/<\omega> = 0.27$).

The expression level of MotA/B was judged by immunoblotting with polyclonal anti-$MotB_C$ antibody. Even in the absence of IPTG, the expression level of MotB(D33N) was 10-fold higher than MotB expressed from the chromosome, and it increased further by adding IPTG (Fig. 2). The rotation of the motor frequently slowed down and/or stopped, but interestingly, the motor speed was restored to the original level after those slowdown and stop events (Fig. 1B–D).

Figure 3 shows that the $\sigma_\omega/<\omega>$ value of the motor containing MotA/B(D33N) significantly increases when the rotation speed is reduced. The wild-type motor stably rotated at about 70 Hz, and the value of $\sigma_\omega/<\omega>$ ranged from 0.1 to 0.2. The rotation rate of the motor containing MotA/B(D33N) ranged from 10 Hz to 50 Hz in the absence of IPTG, and the values of $\sigma_\omega/<\omega>$ were between 0.1 and 0.4. When MotA/B(D33N) was over-expressed by adding IPTG, the motor speed was reduced down to a few hertz, and the value of $\sigma_\omega/<\omega>$ was increased up to 0.5 (Fig. 3). Even in the

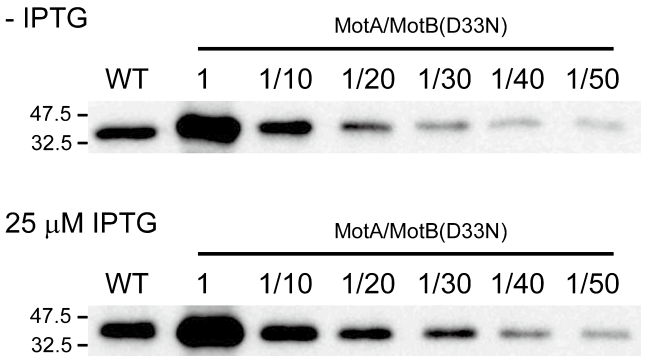

Figure 2 Expression levels of MotA/B(D33N) in comparison with MotA/B by immunoblotting using polyclonal anti-MotB antibody. WT indicates MotB expressed from the chromosome. The fractional values under the label "MotA/B(D33N)" indicate the level of dilution.

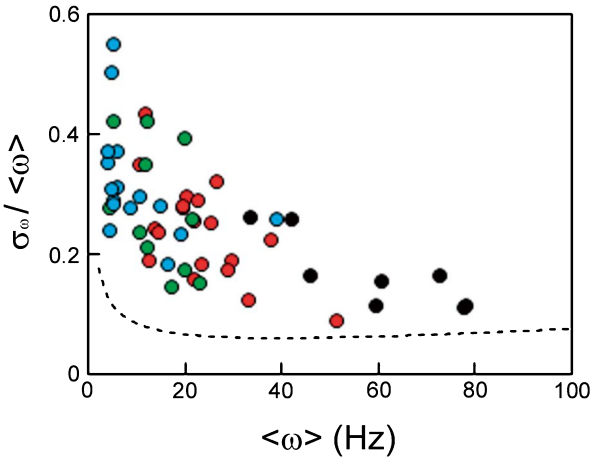

Figure 3 Dependence of the magnitude of fluctuation on the average rotation rate. Cells carrying pNSK9-D33N were grown without IPTG (red), or with 10 μM (green) or 40 μM IPTG (blue). The data from the wild-type *Salmonella* cells carrying a vector plasmid, pTrc99A, are plotted as a control (black). The dashed line shows the fluctuation resulting from the rotational Brownian motion of the flagellar filament with bead and the instrumental uncertainty.

absence of IPTG, the expression level of MotB(D33N) was 10-fold higher than MotB expressed from the chromosome (Fig. 2). As shown in Figure 1, the motor speed fluctuated but never completely stopped for a significant period of time. These observations suggest that the MotA/B(D33N) complex retains the ability to assemble into the motor but with much lower affinity than the MotA/B complex and rapidly dissociates from the motor to be replaced with the wild-type stator.

Computer simulation

To reproduce the speed fluctuation in the presence or absence of the MotA/B(D33N) stator, we used a simple kinetic model proposed by Muramoto *et al*[32]. It was assumed that 11 stators independently function in the motor and that a single wild-type stator unit generates 150 pN nm[18] but the D33N stator unit produces neither positive nor negative torque. The wild-type and D33N stators associate with or dissociate from the rotor with the following rate constants: k_{wt+} and k_{wt-}, association-rate and dissociation-rate constants of the wild-type stator; k_{d33n+} and k_{d33n-}, association-rate and dissociation-rate constants of the D33N stator. The event occurs at an interval of 10^{-4} sec (Δt), and the rotation speed is sampled at an interval of 10^{-3} sec. The association and dissociation probabilities (P_{wt+}, P_{wt-}, P_{d33n-}, and P_{d33n-}) are given as $P_{wt+} = k_{wt+} C_{wt} \Delta t$, $P_{wt-} = k_{wt-} \Delta t$, $P_{d33n+} = k_{d33n+} C_{d33n} \Delta t$, $P_{d33n-} = k_{d33n-} \Delta t$, where C_{wt} and C_{d33n} are the copy number of wild-type stators and D33N stators, respectively. A random number (RND) from 0.0 to 1.0 is generated for each stator unit. For example, if a stator binding position around the rotor is vacant and $P_{wt+} <$ RND, the wild-type stator associates with the rotor and generates torque. If the position is occupied by the wild-type stator and $P_{wt-} <$ RND, the stator dissociates from the rotor and the position becomes vacant.

If $k_{wt+} = k_{d33n+}$ and $k_{wt-} = k_{d33n-}$, the number of wild-type stator units rapidly reduced to zero when the copy number of the D33N stators was 10-fold higher than that of the wild-type stators ($C_{d33n}/C_{wt} = 10$) (Fig. 4A upper panel). In contrast, if $k_{wt+} = k_{d33n+}$ but k_{d33n-} was 10-fold larger than k_{wt-}, the apparent number of stators temporally decreased but was restored even when the copy number of D33N stators was 25-fold higher than that of wild-type stators ($C_{d33n}/C_{wt} = 25$) (Fig. 4A lower panel). The relationship between $<\omega>$ and $\sigma_\omega/<\omega>$ obtained by this simulation is in a relatively good agreement with the present experimental result (Fig. 4B and 3). This suggests that the D33N mutation significantly affects the dissociation constant of the stator unit but not the association constant, to cause the large fluctuation of the motor speed in the presence of both the MotA/B and MotA/B(D33N) complexes. Note that the dissociation constant of the wild-type stator assumed here ($= 0.4\ s^{-1}$) is 10-fold higher than the value predicted from fluorescent observation of GFP-MotB ($\approx 0.04\ s^{-1}$)[23,36]. This raises the possibility that the GFP tag significantly affects the dissociation rate of the MotA/B complex from the motor.

Discussion

The MotA/B complex is assembled into the flagellar motor to be the stator through the binding of the PGB domain of MotB to the PG layer[19–22]. At least 11 stator units can be assembled into the motor, and their association and dissociation are dynamic in response to changes in external load[23–25]. It has been shown that depletion of PMF induces the dissociation of GFP-MotB from the motor in *E. coli*[36]. Consistently, the D32A mutation in *E. coli* MotB interferes with the assembly of GFP-MotB to the flagellar motor[36]. In contrast, the *Salmonella* MotA/B(D33N) complex with totally impaired proton conductivity can still associate with the

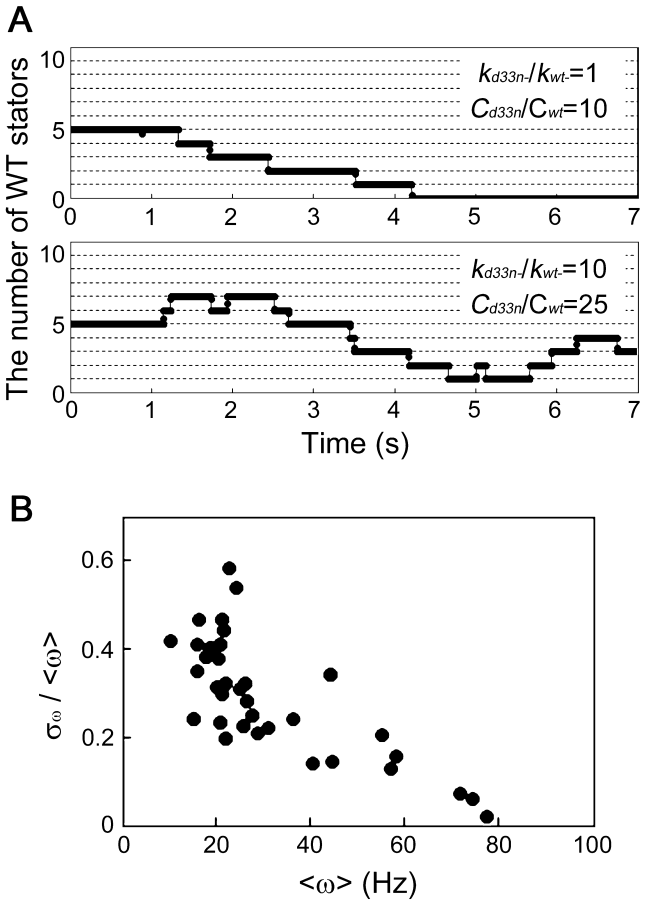

Figure 4 Computer simulation of motor rotation by a dynamic exchange of the wild-type and mutant stators. (A) Temporal change in the number of wild-type stator units at $k_{d33n+}/k_{wt+} = 1$, $k_{d33n-}/k_{wt-} = 1$ and $C_{d33n}/C_{wt} = 10$ (upper panel), and that at $k_{d33n+}/k_{wt+} = 1$, $k_{d33n-}/k_{wt-} = 10$ and $C_{d33n}/C_{wt} = 25$ (lower panel). Initial numbers of wild-type stator units were assumed to be 5. (B) Values of $\sigma_\omega/\langle\omega\rangle$ plotted as a function of $\langle\omega\rangle$ when the value of C_{d33n}/C_{wt} was varied from 0 to 30. The calculation for (B) was done with parameters as follows: $k_{d33n+} = k_{wt+} = 1\,\text{copy}^{-1}\text{s}^{-1}$, $k_{d33n-} = 4\,\text{s}^{-1}$, $k_{wt-} = 0.4\,\text{s}^{-1}$ and $C_{wt} = 200$[23].

rotor and significantly reduces the motor speed when overexpressed in wild-type cells[17]. In agreement with this, depletion of PMF does not abolish the localization of GFP-MotB to the flagellar base[14]. In this study, we showed that a large speed fluctuation of the flagellar motor occurs when both the wild-type and non-functional MotA/B complexes are expressed in *Salmonella* wild-type cells. A high-level expression of the MotA/B(D33N) complex in wild-type cells caused a large speed fluctuation and pausing of motor rotation (Fig. 1).

Several studies concerning unstable rotation of the flagellar motor have been reported to date, and possible sources to generate the speed fluctuation have been proposed as those including the fluctuations in input energy, the number of stator units and the rotational Brownian motion[27,33,34,37,38]. The rate limiting process of proton translocation is thought to limit the maximal motor speed when the motor rotates under low-load conditions, but the effect of proton influx becomes smaller with an increase in the drag force against the motor[9,41]. The motor speed is proportional to the number of stator units under high-load conditions, but just one stator unit can spin the motor at the maximum speed under low-load conditions[18,42,43]. The MotB(D33E) mutation, which reduces the proton influx to about a half of the wild-type MotA/B complex, causes a marked reduction in the maximum motor speed by more than 10 fold and shows a large speed fluctuation only under low load conditions, implying that the stator is a load-sensitive proton channel that efficiently couples proton translocation with torque generation[27].

Since the characteristics of the flagellar motor rotating with a 1-μm bead belong to high-load regime in the torque-speed relationship of *Salmonella*[9], the unstable rotation speed observed in this study is unlikely to be caused by the fluctuation of the proton influx through the MotA/B proton channel. Our present results indicate that the MotA/B(D33N) complex competes with the wild-type MotA/B complex for the stator-binding sites of the motor, associates with the rotor, and reduces the number of functional stator units in a rather dynamic way.

The motors were never completely paralyzed even when the expression level of the MotA/B(D33N) complex reached above 10 fold of the wild-type MotA/B complex (Fig. 2), suggesting that the time period that a MotA/B(D33N) complex occupies a stator binding position is rather short. A computer simulation reproduced the observed speed fluctuations only when the dissociation rate of the MotA/B(D33N) stator was 10-fold higher than that of the wild-type stator, without changing the association rate (Fig. 4). Because the D33N mutation interferes with proton translocation through the proton channel[6,28], we propose that the arrest of proton transduction through the channel suppresses a conformational change or flexibility of the stator required for its stable association with the rotor to make its detachment from the rotor faster. Even in the wild-type motor, when a stator unit becomes malfunctioned during motor rotation, this characteristic may allow the motor to efficiently exchange the broken stator with the functional one.

In our simulation, the stator units were assumed to be independent of each other, and the cooperative association and dissociation of the stator to the motor was not adopted. The simulation reproduced the large fluctuation in the number of functional stators as shown in the experimental results (Fig. 3 and 4A), suggesting that the cooperativity is not really necessary in the mechanism of stator assembly. However, this does not completely eliminate the possibility that a stator dynamics influences its neighbors. To make this clear, direct observation of the stator dynamics around the motor at higher temporal and spatial resolution is required.

Acknowledgement

We thank Y. Sowa for helpful discussion and comments. This research has been supported in part by JSPS KAKENHI Grant 24770141 to S.N., 23115008 on Innovative Areas 'Spying minority in biological phenomena' to T.M. and 21227006 and 25000013 to K.N.

References

1. Berg, H. C. The rotary motor of bacterial flagella. *Annu. Rev. Biochem.* **72**, 19–54 (2003).
2. Kojima, S. & Blair, D. F. The bacterial flagellar motor: structure and function of a complex molecular machine. *Int. Rev. Cytol.* **233**, 93–134 (2004).
3. Sowa, Y. & Berry, R. M. Bacterial flagellar motor. *Q. Rev. Biophys*. **41**, 103–132 (2008).
4. Minamino, T., Imada, K. & Namba, K. Molecular motors of the bacterial flagella. *Curr. Opin. Struct. Biol.* **18**, 693–701 (2008).
5. Morimoto, Y. V. & Minamino, T. Structure and function of the bi-directional bacterial flagellar motor. *Biomolecules* **4**, 217–234 (2014).
6. Zhou, J., Sharp, L. L., Tang, H. L., Lloyd, S. A. & Blair, D. F. Function of protonatable residues in the flagellar motor of *Escherichia coli*: A critical role for Asp32 of MotB. *J. Bacteriol*. **180**, 2729–2735 (1998).
7. Zhou, J., Lloyd, S. A. & Blair, D. F. Electrostatic interactions between rotor and stator in the bacterial flagellar motor. *Proc. Natl. Acad. Sci. USA* **95**, 6436–6441 (1998).
8. Kojima, S. & Blair, D. F. Conformational change in the stator of the bacterial flagellar motor. *Biochemistry* **40**, 13041–13050 (2001).
9. Nakamura, S., Kami-ike, N., Yokota, P. J., Kudo, S., Minamino, T. & Namba, K. Effect of intracellular pH on the torque-speed relationship of bacterial proton-driven flagellar motor. *J. Mol. Biol*. **386**, 332–338 (2009).
10. Braun, T. F., Poulson, S., Gully, J. B., Empey, J. C., Van Way, S., Putnam, A. & Blair, D. F. Function of proline residues of MotA in torque generation by the flagellar motor of *Escherichia coli*. *J. Bacteriol.* **181**, 3542–3551 (1999).
11. Nakamura, S., Morimoto, Y. V., Kami-ike, N., Minamino, T. & Namba, K. Role of a conserved prolyl residue (Pro-173) of MotA in the mechanochemical reaction cycle of the proton-driven flagellar motor of *Salmonella*. *J. Mol. Biol.* **393**, 300–307 (2009).
12. Zhou, J. & Blair, D. F. Residues of the cytoplasmic domain of MotA essential for torque generation in the bacterial flagellar motor. *J. Mol. Biol.* **273**, 428–439 (1997).
13. Zhou, J., Lloyd, S. A. & Blair, D. F. Electrostatic interactions between rotor and stator in the bacterial flagellar motor. *Proc. Natl. Acad. Sci. USA* **95**, 6436–6441 (1998).
14. Morimoto, Y. V., Nakamura, S., Kami-ike, N., Namba, K. & Minamino, T. Charged residues in the cytoplasmic loop of MotA are required for stator assembly into the bacterial flagellar motor. *Mol. Microbiol.* **78**, 1117–1129 (2010).
15. Morimoto, Y. V., Nakamura, S., Hiraoka, K. D., Namba, K. & Minamino, T. Distinct roles of highly conserved charged residues at the MotA-FliG interface in bacterial flagellar motor rotation. *J. Bacteriol.* **195**, 474–481 (2013).
16. Sowa, Y., Rowe, A. D., Leake, M. C., Yakushi, T., Homma, M., Ishijima, A. & Berry, R. M. Direct observation of steps in rotation of the bacterial flagellar motor. *Nature* **437**, 916–919 (2005).
17. Nakamura, S., Kami-ike, N., Yokota, J. P., Minamino, T. & Namba, K. Evidence for symmetry in the elementary process of bidirectional torque generation by the bacterial flagellar motor. *Proc. Natl. Acad. Sci. USA* **107**, 17616–17620 (2010).
18. Reid, S. W., Leake, M. C., Chandler, J. H., Lo, C.-J., Armitage, J. P. & Berry, R. M. The maximum number of torque-generating units in the flagellar motor of *Escherichia coli* is at least 11. *Proc. Natl. Acad. Sci. USA* **103**, 8066–8071 (2006).
19. De Mot, R. & Vanderleyden, J. The C-terminal sequence conservation between OmpA-related outer membrane proteins and MotB suggests a common function in both gram-positive and gram-negative bacteria, possibly in the interaction of these domains with peptidoglycan. *Mol. Microbiol.* **12**, 333–334 (1994).
20. Kojima, S., Furukawa, Y., Matsunami, H., Minamino, T. & Namba, K. Characterization of the periplasmic domain of MotB and implications for its role in the stator assembly of the bacterial flagellar motor. *J. Bacteriol.* **190**, 3314–3322 (2008).
21. Roujeinikova, A. Crystal structure of the cell wall anchor domain of MotB, a stator component of the bacterial flagellar motor: Implications for peptidoglycan recognition. *Proc. Natl. Acad. Sci. USA* **105**, 10348–10353 (2008).
22. Kojima, S., Imada, K., Sakuma, M., Sudo, Y., Kojima, C., Minamino, T., Homma, M. & Namba, K. Stator assembly and activation mechanism of the flagellar motor by the periplasmic region of MotB. *Mol. Microbiol*. **73**, 710–718 (2009).
23. Leake, M. C., Chandler, J. H., Wadhams, G. H., Bai, F., Berry, R. M. & Armitage, J. P. Stoichiometry and turnover in single, functioning membrane protein complexes. *Nature* **443**, 355–358 (2006).
24. Lele, P. P., Hosu, B. G. & Berg, H. C. Dynamics of mechanosensing in the bacterial flagellar motor. *Proc. Natl. Acad. Sci. USA* **110**, 11839–11844 (2013).
25. Tipping, M. J., Delalez, N. J., Lim, R., Berry, R. M. & Armitage, J. P. Load-dependent assembly of the bacterial flagellar motor. *MBio* **4**, e00551–13 (2013).
26. Castillo, D. J., Nakamura, S., Morimoto, Y. V., Che, Y-S., Kami-ike, N., Kudo, S., Minamino, T. & Namba, K. The C-terminal periplasmic domain of MotB is responsible for load-dependent control of the number of stators of the bacterial flagellar motor. *BIOPHYSICS* **9**, 173–181 (2013).
27. Che, Y.-S., Nakamura, S., Morimoto, Y. V., Kami-ike, N., Namba, K. & Minamino, T. Load-sensitive coupling of proton translocation and torque generation in the bacterial flagellar motor. *Mol. Microbiol.* **91**, 175–184 (2014).
28. Morimoto, Y. V., Che, Y-S., Minamino, T. & Namba, K. Proton-conductivity assay of plugged and unplugged MotA/B proton channel by cytoplasmic pHluorin expressed in *Salmonella*. *FEBS Lett.* **584**, 1268–1272 (2010).
29. Yoshioka, K., Aizawa, S-I. & Yamaguchi, S. Flagellar filament structure and cell motility of *Salmonella typhimurium* mutants lacking part of the outer domain of flagellin. *J. Bacteriol*. **177**, 1090–1093 (1995).
30. Minamino, T., Imae, Y., Oosawa, F., Kobayashi, Y. & Oosawa, K. Effect of intracellular pH on rotational speed of bacterial flagellar motors. *J. Bacteriol.* **185**, 1190–1194 (2003).
31. Che, Y-S., Nakamura, S., Kojima S., Kami-ike, N., Namba, K. & Minamino, T. Suppressor analysis of the MotB(D33E) mutation to probe the bacterial flagellar motor dynamics coupled with proton translocation. *J. Bacteriol.* **190**, 6660–6667 (2008).
32. Muramoto, K., Magariyama, Y., Homma, M., Kawagishi, I., Sugiyama, S., Imae, Y. & Kudo, S. Rotational fluctuation of the sodium-driven flagellar motor of *Vibrio alginolyticus* induced by binding of inhibitors. *J. Mol. Biol.* **259**, 687–695 (1996).

33. Khan, S., Meister, M. & Berg, H. C. Constraints on flagellar rotation. *J. Mol. Biol.* **184**, 645–656 (1985).
34. Muramoto, K., Kawagishi, I., Kudo, S., Magariyama, Y., Imae, Y. & Homma, M. High-speed rotation and speed stability of the sodium-driven flagellar motor. *J. Mol. Biol*. **251**, 50–58 (1995).
35. Minamino, T. & Macnab, R. M. Components of the *Salmonella* flagellar export apparatus and classification of export substrates. *J. Bacteriol*. **181**, 1388–1394 (1999).
36. Tipping, M. J., Steel, B. C., Delalez, N. J., Berry, R. M. & Armitage, J. P. Quantification of flagellar motor stator dynamics through in vivo proton-motive force control. *Mol. Microbiol.* **87**, 338–347 (2013).
37. Eisenbach, M., Wolf, A., Welch, M., Caplan, S. R., Lapidus, I. R., Macnab, R. M. Aloni, H. & Asher, O. Pausing, switching and speed fluctuation of the bacterial flagellar motor and their relation to motility and chemotaxis. *J. Mol. Biol*. **211**, 551–563 (1990).
38. Samuel, A. D. T. & Berg, H. C. Fluctuation analysis of rotational speeds of the bacterial flagellar motor. *Proc. Natl. Acad. Sci. USA* **92**, 3502–3506 (1995).
39. Kara-Ivanov, M., Eisenbach, M. & Caplan, S. R. Fluctuations in rotation rate of the flagellar motor of *Escherichia coli*. *Biophys. J.* **69**, 250–263 (1995).
40. Samuel, A. D. T. & Berg, H. C. Torque-generating units of the bacterial flagellar motor step independently. *Biophys. J.* **71**, 918–923 (1996).
41. Chen, X. & Berg, H. C. Solvent-isotope and pH effects on flagellar rotation in *Escherichia coli*. *Biophys. J.* **78**, 2280–2284 (2000).
42. Ryu W. S., Berry, R. M. & Berg, H. C. Torque-generating units of the flagellar motor of *Escherichia coli* have a high duty ratio. *Nature* **403**, 444–447 (2000).
43. Yuan, J. & Berg, H. C. Resurrection of the flagellar rotary motor near zero load. *Proc. Natl. Acad. Sci. USA* **105**, 1182–1185 (2008).